Probiotics Ameliorate Alveolar Bone Loss by Regulating Gut Microbiota

Leming Jia
West China School of Stomatology, Sichuan University
Ye Tu
West China School of Stomatology, Sichuan University
Xiaoyue Jia
West China School of Stomatology, Sichuan University
Qian Du
West China School of Stomatology, Sichuan University
Xin Zheng
West China School of Stomatology, Sichuan University
Quan Yuan
West China School of Stomatology, Sichuan University
Liwei Zheng
West China School of Stomatology, Sichuan University
Xuedong Zhou
West China School of Stomatology, Sichuan University
Xin Xu (xin.xu@scu.edu.cn)
West China School of Stomatology, Sichuan University https://orcid.org/0000-0003-4608-4556

Research

Keywords: alveolar bone loss, probiotics, estrogen deficiency, intestinal barrier, osteoimmunology, Th17 cell, Treg cell

Posted Date: October 28th, 2020

DOI: https://doi.org/10.21203/rs.3.rs-97356/v1

Abstract

Background

Estrogen deficiency is an etiological factor of postmenopausal osteoporosis (PMO), which not only decreases bone density in vertebrae and long bone, but also aggravates inflammatory bone loss in alveolar bone. Recent evidence has suggested the critical role of gut microbiota in osteoimmunology, and modulation of gut microbiota may have positive influence on bone metabolisms. The present study aimed to evaluate the therapeutic effects of probiotics on alveolar bone loss under estrogen-deficient condition. Inflammatory alveolar bone loss induced by either chronic periodontitis or apical periodontitis was established in ovariectomized (OVX) rats, which were gavage-fed with probiotics daily until sacrifice. Gut microbiota and gut permeability, as well as alveolar bone loss and the related osteoimmune were evaluated to investigate the effects and underlying mechanisms by which probiotics counter the alveolar bone loss under estrogen-deficiency.

Results

We found that administration of probiotics significantly prevented periodontal and apical bone resorption in OVX rats. Administration of probiotics significantly enriched butyrate-producing genera and enhanced gut butyrate production, resulting in improved intestinal barrier and decreased gut permeability in the OVX rats. Furthermore, the estrogen deprivation-induced inflammatory responses were suppressed in probiotics-treated OVX rats, as reflected by reduced serum levels of inflammatory cytokines and a balanced distribution of $CD4^+$IL-$17A^+$Th17 cells and $CD4^+CD25^+Foxp3^+$Treg cells in the bone marrow.

Conclusion

Our data demonstrate that probiotics can effectively attenuate alveolar bone loss by modulating gut microbiota and further regulating osteoimmune, and thus represent a promising adjuvant in the treatment of alveolar bone loss under estrogen-deficiency.

Background

Osteoporosis is a systematic bone disorder characterized by decreased bone mineral density (BMD) and compromised bone microarchitecture, leading to an increased risk of bone fracture[1]. Postmenopausal osteoporosis (PMO) is the most common type of osteoporosis mainly caused by the cessation of ovarian function[1, 2]. Aberrant immune response has been linked to the etiology of PMO, and PMO has been proposed as a chronic inflammatory disease[2-4]. Estrogens play pivotal roles in stimulating osteoblast lifespan and suppressing osteoclast differentiation[1, 5]. Estrogen-deficiency results in immune dysregulation, characterized with a skewed distribution and enhanced activity of Th17 cells ($CD4^+$IL-$17A^+$cells)[6]. Th17 cells function as an osteoclastogenic subset of T helper cells that promote the release of osteoclastogenic cytokines, such as RANKL, TNF-α, and IL-17[2, 6]. Elevated levels of circulating IL-17 have been reported in either ovariectomized (OVX) mice or postmenopausal women[7-9].

IL-17 triggers osteoclastogenesis and simultaneously stimulates RANKL, TNF-α and IL-6 expression[7, 10, 11]. Recent studies have demonstrated the close involvement of IL-17 not only in the development of PMO but also the progression of inflammatory arthritis and alveolar bone loss[7, 12-14].

Chronic periodontitis (CP) and apical periodontitis (AP) are polymicrobial infectious disease characterized with local inflammatory response within the supporting tissue of teeth, leading to alveolar bone loss[15, 16]. Despite the common lesion of osteoporosis in long bones and vertebras, many studies have reported the exacerbate alveolar bone resorption under estrogen-deficiency[17-20], imposing challenges to the clinical treatment of these diseases. Conventional therapies of CP and AP mainly rely on mechanical removal of plaque biofilm and root canal therapy. However, poor clinical treatment outcome has been noted in the elder women with PMO[21-23]. The traditional PMO drugs such as bisphosphonates and RANK ligand inhibitor have been demonstrated effective on inhibiting osteoclast activity[24], but with non-negligible adverse effects such as medication-related osteonecrosis of the jaw (MRONJ)[25, 26], limiting their routine use as an adjuvant treatment of CP and AP.

Increasing evidence has indicated a close association between gut microbiota and bone metabolism, and the gut-bone axis has been proposed[27-29]. Aberrant gut microbiota is associated with decreased BMD and osteopenia[30, 31]. In addition, the estrogen-depleted germ-free mice present decreased expression of TNF-α, RANKL, and IL-17 and increased BMD as compared to the SPF mice[8, 32], further underlining the critical roles of gut microbiota in skeletal homeostasis. Modulation of gut microbiota has been proposed as a potential approach to the management of skeletal disorders[29]. Probiotics are live microorganisms which confer a health benefits on the host mainly via modulating gut microbiota[33]. Probiotics have demonstrated effectiveness in the treatment of inflammatory bowel disease (IBD), irritable bowel syndrome (IBS), antibiotic-associated diarrhea, and necrotizing enterocolitis[34]. Recent studies have also demonstrated the protective effects of probiotics towards bone[8, 35, 36]. Probiotics *Lactobacillus rhamnosus GG* and commercially available probiotics supplement VSL #3 dampens bone mineral inflammation and completely protest against bone loss[8]. Although specific mechanisms are still unclear, oral administration of *Lactobacillus rhamnosus GG*, *Bifidobacterium animalis subsp. Lactis*, and *Akkermansia muciniphila* have shown the effectiveness in suppressing alveolar bone loss and reducing the severity of CP and AP in animal models[37-40]. Our previous work showed that berberine, a natural alkaloid, was able to ameliorate periodontal bone loss by regulating gut microbiota of OVX rats[41], underscoring the importance of gut microbiota modulation in the reversion of alveolar bone resorption. To further delineate the mechanism by which probiotics ameliorate alveolar bone loss, we hypothesize that probiotics can promote the intestinal barrier function by modulating gut microbiota, subsequently alleviate osteoimmune response, and consequently ameliorate periodontal and apical bone loss under estrogen deficiency. To validate this hypothesis, we administered probiotics to the OVX rats with either CP or AP, and investigated the effect of gavage-feeding of probiotics on the inflammatory alveolar bone loss. The effect of probiotics on gut barrier and osteoimmune response were further explored to delineate the underlying mechanisms.

Results

Probiotics restore the gut permeability of OVX rats by enriching butyrate-generating bacteria

Principal components analysis (PCA) and principal coordinates analysis (PCoA) based on Bray-Curtis distance showed significant alteration of gut microbiota on operational taxonomic unit (OTU) level in OVX rats, and the altered microbial community structure was reversed by the administration of probiotics (Figure1a). More importantly, gavage-feeding of probiotics significantly elevated the levels of butyrate-producing genera that were deprived in OVX rats, including *Clostridium leptum* subgroup, *Clostridium coccoides* subgroup, *Fecalibacterium prausnitzii,* and *Roseburia/E.rectale cluste* (Figure 1b). Consistently, we found that transcripts encoding butyrate synthesis-associated enzymes, including butyryl-CoA:acetate CoA transferase (*But*) and butyrate kinase (*Buk*) were downregulated in the OVX rats, and the administration of probiotics significantly upregulated *But* and *Buk* expression (Figure 1c). In parallel, the scarcity in butyrate as observed in the intestine of OVX rats was reversed by the gavage-feeding of probiotics (Figure 1d).

Further morphologic analyses of the intestinal villi showed no significant difference of intestinal crypt depth (ICD) in the OVX rats as compared to the sham-operated controls (Figure 2b). However, significant decrease in intestinal villus height (IVH), intestinal villus density (IVD), as well as V/C value was observed in OVX rats as compared to the sham-operated rats (Figure 2c-e), suggesting a compromised gut barrier (Figure 2a). More importantly, gavage-feeding of probiotics effectively improved the intestinal barrier of the OVX rats via restoring the normal morphology of intestinal villi as reflected by IVH, IVD and V/C value (Figure 2a, c-e).

The gut permeability of the OVX rats was further evaluated. qPCR data showed a decreased expression of TJ protein-encoding genes, including Occludin, Claudin1, Claudin1, Claudin3, ZO1, JAM3 in the intestinal epithelia of OVX rats, and administration of probiotics significantly upregulated the expression of these TJ proteins-related genes (Figure 2f). Serum levels of FITC-dextran and LPS were further measured to evaluate the intestinal paracellular permeability. Consistently, elevated levels of serum FITC-dextran and LPS were observed in OVX rats as compared to the sham-operated controls (Figure 2g-h), suggesting an enhanced gut permeability under estrogen-deficiency. Gavage-feeding of probiotics promoted the gut barrier in the OVX rats as reflected by the decreased leakage of FITC-dextran and LPS (Figure 2g-h). In addition, gavage-feeding of exogenous butyrate upregulated the expression of TJ proteins and decreased the intestinal leakage of FITC-dextran in OVX rats (Supplemental Figure 1a, b), further suggesting that butyrate is critical for gut permeability, and probiotics protect the gut barrier of OVX rats likely by enriching the butyrate-generating bacteria.

Probiotics alleviate bone resorption and normalize aberrant osteoimmune response in OVX rats

Micro-CT analyses of the femoral cancellous bone of the OVX rats showed a typical osteoporosis phenotypes, as reflected by the decrease in bone volume per tissue (BV/TV), trabecular number (Tb.N), trabecular separation (Tb.Sp), and increase in trabecular bone pattern factor (Tb.Pf) (Figure 3a-e).

Administration of probiotics significantly rescued the bone loss of OVX rats (Figure 3a-e), and the complex-probiotic showed better protective effects as compared to the single strain of *Bifidobacterium longum* BL986 and *Lactobacillus rhamnosus* LRH09 (Supplemental Figure 2a-e).

Analysis of serum inflammatory cytokines showed an increased level of IL-17A and TNF-α in the OVX rats as compared to the sham-operated controls, and gavage-feeding of probiotics countered the elevation of these osteoclastogenic cytokines (Figure 3f, g). We further analyzed the osteoimmune response with flowcytometry. A skewed distribution of Th17/Treg cells in the bone marrow of OVX rats was observed as reflected by a higher frequency of Th17 cells (Figure 3h) and lower frequency of Treg cells (Figure 3i). Gavage-feeding of probiotics effectively reconstituted the Th17/Treg balance by decreasing the proportion of Th17 cells (Figure 3h) and increasing Treg cells, respectively (Figure 3i). In addition, exogenous butyrate treatment also rescued the Treg/Th17 imbalance (Supplemental Figure 3a, b), further suggested the linkage between gut permeability and abnormal osteoimmune response.

Probiotics ameliorates periodontal bone loss in OVX rats

The effects of estrogen-deficiency and probiotics treatment on the periodontal bone resorption were further investigated. Estrogen-deficiency exacerbated the alveolar bone resorption in periodontitis (Figure 4a-c), resulting in decreased BV/TV, Tb.N, Tb.Sp, and increased Tb.Pf in the alveolar bone (Figure 4d-g). Administration of probiotics significantly ameliorated periodontal bone loss of OVX rats (Figure 4a-g), and the complex-probiotic showed better protective effects as compared to the single strain of *Bifidobacterium longum* BL986 and *Lactobacillus rhamnosus* LRH09 (Supplemental Figure 4). Further histological analyses showed an increased $TRAP^+$ osteoclasts and reduced $osteocalcin^+$ osteoblasts per bone surface in the OVX/CP rats as compared to the sham/periodontitis controls, suggesting an active periodontal bone resorption under estrogen-deficiency (Figure 5a, b). Probiotics treatment significantly countered the elevated activity of bone resorption by decreasing the number of $TRAP^+$ cells increasing OCN^+ cells in the alveolar bone (Figure 5a, b). Furthermore, an increased number of $IL\text{-}17A^+$ cells and decreased $Foxp3^+$ cells per bone surface were observed in OVX/CP rats, and this skewed $CD4^+$ T cells-mediated osteoimmune response were rescued by the administration of probiotics (Figure 5c, d).

Probiotics ameliorates apical bone loss in OVX rats

The apical periodontitis rat model was further established to investigate the effect of estrogen-deficiency and probiotics on the inflammatory alveolar bone loss. Estrogen-deficiency aggravated alveolar bone loss in apical bone region (Figure 6a-c), while oral gavage of probiotics effectively ameliorated the apical bone loss of OVX rats (Figure 6a-c). Further histological analyses showed a resorption-dominant condition in the apical bone region of OVX/AP rats, as reflected by increased $TRAP^+$ osteoclasts and decreased $osteocalcin^+$ osteoblasts per high-power field (hpf) (Figure 7a, b). Administration of probiotics significantly reversed the apical bone resorption by reducing the number of $TRAP^+$ cell and elevating OCN^+ cells (Figure 7a, b). Moreover, the skewed distribution of Th17/Treg cells in the apical bone region

of OVX/AP rats was also rescued by the treatment of probiotics, as reflected by decreased IL-17A$^+$ cells and increased Foxp3$^+$ cells per hpf (Figure 7c, d).

Discussion

Chronic periodontitis and apical periodontitis are common oral diseases that cause gradual loss of alveolar bone and consequently tooth loss. Poor oral hygiene and systemic diseases such as diabetes and postmenopausal osteoporosis predispose individuals to the development and progression of these diseases. More importantly, diabetes and PMO can compromise the clinical outcome of conventional treatment such as oral prophylaxis and root canal therapy[42-44], imposing challenges on the clinical management of these diseases, particularly in the population of elder women. The current study demonstrated that probiotics can ameliorate the alveolar bone loss in estrogen-deficient rats via modulating the gut microbiota, and thus represent a promising adjuvant to the treatment of CP and AP.

Recent studies have revealed the critical role of Th17/Treg balance in the bone loss of PMO[45]. Th17 cells are a subset of proinflammatory T helper cells that potently induce the differentiation of osteoclasts by releasing IL-17A, RANKL, TNF, and IL-6 [46, 47], consequently leading to bone destruction. Increased differentiation of Th17 cells and circulating IL-17 levels have been observed in OVX mice and postmenopausal women[7-9]. Neutralization of IL-17A significantly prevents bone loss induced by estrogen-deficiency via coupling the bone-remodeling process[48]. On the other hand, estrogen can promote the differentiation of Treg cells[49, 50], which is an immunosuppressive CD4$^+$ T cell subsets mediating the tolerance to autoimmune and maintaining the immune homeostasis[51]. Treg cells have been reported effectively inhibited the osteoclastogenesis via secreting TGF-β, IL-4, and IL-10[4, 52]. Treg can also induce the activation of enzyme indoleamine 2,3-dioxygenase (IDO), initiating the apoptosis of osteoclast precursors via the cell-cell contact mediated by cytolytic T lymphocyte associated antigen-4 (CTLA-4)[53]. The skewed distribution of Th17/Treg cells has been identified in the pathogenesis of PMO, as well as in other inflammatory diseases such as periodontal and apical diseases. Function of Th17 and Treg is closely connected with bone metabolism[46, 54]. Restoration of Th17/Treg balance has been proven effective in the management of CD4$^+$ T cells-mediated bone loss[55]. The current study also identified skewed distribution of Th17/Treg cells as reflected by increased Th17 cells and decreased Treg cells in the bone marrow of OVX rats, and gavage-feeding of probiotics can effectively rescue this CD4$^+$ T cells abnormality, consequently attenuating the alveolar bone loss as observed in either periodontitis or apical periodontitis.

Recent studies have shown that the translocation of gut microbiota and/or its metabolites provides necessary antigens required for T cells activation in the bone marrow, inducing bone loss in estrogen-deficiency[8]. The regulatory role of gut microbiota in osteoimmune has been recognized. In germ-free mice, estrogen deprivation failed to stimulate the osteoclastogenic cytokines and initiate the bone resorption[8]. Components derived from gut microbiota, especially lipopolysaccharides (LPS), is a potent inflammatory inducer by activating Toll-like receptors 4[56, 57]. On the other hand, the short chain fatty

acids (SCFAs) produced by gut microbiota play an importantly role in the maintenance of epithelial barrier functions[58, 59]. SCFAs also suppress the differentiation of Th17 cells, and reduce the production of osteoclastogenic cytokines including IL-6, IL-17 and IL-23[60, 61]. In addition, SCFAs can induce the differentiation of colonic Treg cells via SCFA-receptor FFAR2 (GPR43) and histone deacetylase (HDAC)-inhibitory activity, thus suppressing the mucosal inflammation[62, 63]. Promoting gut-derived SCFAs generation has shown protective effects in multiple diseases including IBS, cardiovascular diseases, Alzheimer's disease and rheumatoid arthritis[58, 64-66]. Probiotics have been shown to increase intestinal SCFAs levels and promote gut barrier function[63, 67-69]. More importantly, probiotics have been reported to increase the BMD[27]. Probiotics can promote the absorption of bone formation-related minerals[70, 71]. suppress $CD4^+$ T cells in bone marrow and protect bone loss induced by estrogen-deficiency[72]. Administration of probiotics can also elevate Treg cells in the bone marrow of OVX mice, and thus suppress bone loss[73, 74]. Although mechanisms are still unclear, beneficial local effects of probiotics on inflammatory alveolar bone loss have also been reported[38, 75-77]. Our previous study also shown that administration of berberine, a natural alkaloid with well-known ecological effect on gut microbiota, can enrich butyrate-generating bacteria and elevate the generation of gut-derived SCFAs, which promote gut barrier function and attenuate OVX-exacerbated periodontal bone loss[41]. Consistently, our current work found that the dysbiotic gut microbiota under estrogen-deficiency increased gut permeability with enhanced serum LPS, and the ensuing inflammatory responses skewed the distribution of Th17/Treg cells in the bone marrow and aggravated alveolar bone loss. Probiotics can reconstitute the structure of gut microbiota, particularly enrich butyrate-generating bacteria and enhance the production of SCFAs, which promote gut barrier function and subsequently restore the Th17/Treg balance, and consequently ameliorate alveolar bone loss both in either periodontal and apical diseases.

Of note, the current study showed that gavage-feeding of probiotics exerted no positive effects on the alveolar bone destruction in rats free of OVX or inflammatory state. This is consistent with our previous findings of berberine or probiotics treatment outcome reported by others[41, 78]. This may suggest the unnecessity of over-supplementation of probiotics in healthy population as also suggested by many researchers[79, 80]. Besides, the regulatory effects of probiotics on gut-derived estrogens have been suggested, further suggesting its application to the combinatory management of osteoporosis and alveolar bone loss in postmenopausal women[81].

Conclusion

Our current work shows that estrogen-deficiency increases gut permeability with dysbiotic microbiota, and the ensuing systemic inflammatory response skews Th17/Treg distribution and consequently aggravates alveolar bone loss in periodontal diseases and apical diseases. Probiotics can reconstitute gut microbiota and promote gut barrier function, restore Th17/Treg balance, and consequently ameliorate alveolar bone loss. Probiotics may represent a promising adjuvant therapeutics to the combinatory management of PMO and periodontal/apical bone loss in elder women.

Methods

Animals and experimental design

10-Week-old Sprague-Dawley female rats (Da Shuo, China) were housed under specific pathogen-free condition. After acclimatization for 1 week, rats were intraperitoneally anaesthetized by pentobarbital sodium (2%, 40mg/kg), and bilaterally ovariectomized or subjected to sham surgery. Rats were then treated with probiotics or vehicle. Rats were supplemented by oral gavage with $1X10^7$ CFU/day commercially available infant probiotics preparation that contains 10 single strains including *Lactobacillus rhamnosu* HN001, *Bifidobacterium lactis* BI-04, *Bifidobacterium animals* HN019, *Lactobacillus fermentium* SBS-1, *Lactobacillus reuteri* 1e1, *Bifidobacterium longum* BB536, *Bifidobacterium breve* M16-V, *Bifidobacterium infantis* Bi-26, *Lactobacillus paracasei* Lpc-37 (lifespace, Australia, later referred to as lsPro) or single strain probiotics *Bifidobacterium longuBL986* and *Lactobacillus* rhamnosus LRH09 until sacrifice. CP or AP were induced three weeks after ovariectomy/sham operation. The CP rat model was established according to the methods described by Li and Amar with minor modifications[82]. Rats were intraperitoneally anaesthetized by pentobarbital sodium (2%, 40mg/kg) and were ligated with a 5-0 silk suture around the bilateral maxillary first molars to establish experimental periodontitis. *P. gingivalis* ATCC 33277, which was anaerobically grown and resuspended to a concentration of 1×10^7 CFU/mL in saline, was smeared on the silk suture every 3 days after ligation[41]. The AP rat model was established as reported by Brasil with minor modifications[20]. The tooth pulps of bilateral mandibular first molars were exposed to oral environment through the occlusal surface using micro-round bur in a high-speed motor, leading to a spontaneous development of apical periodontitis.

Specimens collection

Four weeks after ligation or pulp exposure, samples of the rats were collected. Feces were collected in 1.5-ml sterile Eppendorf tubes, and immediately stored at -80℃. Blood samples were collected from the abdominal aorta under intraperitoneal anesthesia. Rats were then sacrificed by cervical dislocation. 2-cm segments of ileum from all rats were immediately excised and submerged into 1 mL of TriZol reagent for RNA isolation. Bilateral maxilla from rats representing periodontitis, bilateral mandibles from rats representing AP and 2-cm segments ileum from all rats were removed and fixed in 4% paraformaldehyde for 24 hours. Femurs were dissected thoroughly free from soft tissue. The tips of the femurs were removed and bone marrow (BM) was harvested by inserting a syringe needle into one end of the bone and flushing with phosphate-buffered saline (PBS).

Micro-CT scanning and analysis

To evaluate the bone destruction and micro-architecture of alveolar bone and femur bone, micro-CT was performed as previously described with minor modifications[41, 83, 84]. Fixed bone specimens were placed in an airtight cylindrical sample holder and scanned with a micro-CT (μCT50; SCANCO). The micro-CT images were imported into CT-Analyser software (version 1.13, Bruker, Kontich, Belgium) to

qualitatively depict the alveolar bone loss and perform histomorphometric analysis of trabecular bone. As for alveolar bone, the scanning was performed at 70 kV and 200 mA with 300-millisecond integration time. All samples were scanned in the sagittal position at a voxel resolution of 10μm. As for rats with CP, mesial and distal bone loss of maxilla was quantified by measuring the average distance between the alveolar bone crest and the cemento-enamel junction (CEJ) with sagittal images selected in the middle of the maxillary first molar. 60 continuous sagittal images of the alveolar bone at root furcation, starting at the beginning of trabecular bone without the middle root, were selected for the analysis of trabecular bone at the region of interest (ROI). For each image, the ROI was a rectangular region of 5.2 mm^2 defined right below the top of bone septum between mesial and distal roots. The trabecular parameters of bone volume per tissue volume (BV/TV), Trabecular Number (Tb.N), trabecular separation (Tb. Sp) and Trabecular bone pattern factor (Tb. Pf) at the ROI were measured and quantified. As for rats with AP, the volume of bone resorption cavities under the mesial root of mandibular first molar was quantified. Femurs were also scanned at 70 kV and 200 mA with 300-millisecond integration time in the transverse position at a voxel resolution of 12.5μm. 50 continuous images of the site near femoral condylar in horizontal directions were selected for trabecular bone analyses, and the trabecular parameters of BV/TV, Tb. N, Tb. Sp and Tb. Pf at the ROI were measured and quantified. The micro-CT scanning and measurements were performed blindly by one experienced doctor.

Analysis of serum proinflammatory cytokine

Serum was isolated by centrifuging the blood after clotting at 4,000 rpm for 10 min. The serum levels of TNF-α and IL-17A were assayed by ELISA kits (Invitrogen) according to the manufacturer's directions.

Histologic analyses of alveolar bone and ileum tissue

Histologic analyses were performed with the method previously described with minor modification[41, 84]. Alveolar bone loss at root furcation for periodontitis and apical destruction surrounding the mesial root of mandibular first molar for apical periodontitis was examined by hematoxylin and eosin (H&E) staining.

Osteoclasts in alveolar bone were examined by tartrate-resistant acid phosphatase (TRAP) staining using the Acid Phosphatase Leukocyte kit (Sigma, St. Louis, MO). Osteocalcin$^+$ (OCN) cells, Foxp3$^+$ cells and IL-17A$^+$ cells in the alveolar bone were examined by immunohistochemistry (IHC) using specific primary antibodies (OCN, ab13420, Abcam; Foxp3, ab22510, Abcam; IL-17A, ab136668, Abcam) and anti-mouse HRP-DAB cell&tissue staining kit (CTS002, R&D) or anti-rabbit HRP-DAB cell&tissue staining kit (CTS005, R&D systems). As for the quantification of positively stained cells in the alveolar bone of CP, six high power fields (hpf) (× 400) at ROI were randomly selected, and the positively stained cells were enumerated by Image-Pro Plus (IPP, Media Cybernetics, USA). Data were presented as the number of positively stained cells per square millimeter of bone marrow. As for the quantification of positively stained cells in the alveolar bone of AP, areas selected for cell enumeration were defined as those centered at a fixed distance from the mesial root apical foramen. Positively stained cells from 5 randomly

selected areas at the apical region were counted under hpf (×400) magnification, and data were presented as the number of positively stained cells per hpf.

Intestinal barrier integrity was also examined by H&E staining. Images captured at ×100 magnification were randomly selected, and morphologic features of intestinal villi including intestinal villus density (1/mm), intestinal villus height (mm), intestinal crypt depth (mm), and the ratio of villus height to crypt depth (V/C) were evaluated by IPP.

16S rRNA sequencing of gut microbiota

Genomic DNA was extracted and purified from feces (3-5g) with the QIAamp DNA stool mini kit (QIAGEN). The resulting DNA was quantified with Quant-iTTM PicoGreen reagent (Invitrogen). The sequencing of 16S rRNA amplicons (V1-V3 region) was performed by MiSeq 300PE (Illumina MiSeq System) at Majorbio (Shanghai, China). Primers used in present study was 27F (5'-AGAGTTTGATCCTGGCTCAG-3') and 533R (5'-TTACCGCGGCTGCTGGCAC-3'). A total of 151465 sequence reads of feces were generated from the amplicon library, with an average of 12624 reads per sample. The sequences were clustered into 850 operational taxonomic units (OTU) in feces at a similarity level of 97%. Bioinformatics were performed by Mothur and QIIME2.0 software, including quality control of raw data, taxonomic annotation based on the Silva database, taxonomy-based comparisons at the OTU level, β-diversity analysis including principal component analysis (PCA) and principal coordinates analysis (PCoA), dissimilarity analyses including analysis of similarity (ANOSIM) and non-parametric multivariate analysis of variance (Adonis). The sequencing raw data were deposited in Sequence Read Archive (https://www.ncbi.nlm.nih.gov/Traces/sra; accession nos. SRP285657).

Fecal butyrate quantification

Fresh feces (10 mg per rat) were processed by the ether extraction method. A 20-μL volume of the prepared sample solution was analyzed by a high-performance liquid chromatography (HPLC) system (model 1260; Agilent) with an HPLC column (4.0 mm × 250 mm, 5 μm, InertSustain C18; SHIMADUZ-GL). The mobile phases were 0.2% H_3PO_4 solution (A phase) and methanol (B phase; Chromatographic Grade; Fisher Scientific), with a flow rate of 0.8 mL/min and a column temperature of 30 °C. HPLC was performed with binary solvent–delivery gradient elution with a detection wavelength of 210 nm.

RNA isolation and quantitative reverse transcription polymerase chain reaction

Intestinal RNA was isolated and purified from an ileum segment with TriZol Reagent (Invitrogen). Reverse transcription of RNA into cDNA was performed with the Primer-Script RT Reagent Kit with gDNA Reaser (RR047A; Takara Bio). The expression of genes encoding intestinal tight junction (TJ) proteins, including occludin, zo-1, claudin1, claudin 2, claudin 3, and Jam3, were quantified with the β-actin as internal control. The primer sequences are presentedin Table 1. Relative quantitative analysis was performed with the $2^{-\Delta\Delta CT}$ method.

Fecal RNA was isolated and purified with stool RNA kit (R6828-01; OMEGA bio-tec). Reverse transcription of RNA into cDNA was performed with the Primer-Script RT Reagent Kit with gDNA Reaser (RR047A; Takara Bio). The expression levels of butyryl-CoA:acetate CoA transferase (*But*) and butyrate kinase (*Buk*) of the gut microbiota were measured with the 16S rRNA gene as internal control. The primer sequences are presented in Table 2. Relative quantitative analysis was performed with the $2^{-\Delta\Delta CT}$ method. As for the measurement of butyrate producing genera, fecal DNA was isolated and purified with stool DNA kit (QIAamp DNA stool mini kit, QIAGEN). The relative abundance of *Clostridium leptum* subgroup, *Clostridium coccoides* subgroup, *Fecalibacterium prausnitzii*, and *Roseburia/E. rectale cluster* were measured with the 16s-univ-1 gene as internal control. The primer sequences are presented in Table 3. Relative quantitative analysis was performed with the $2^{-\Delta\Delta CT}$ method.

Intestinal permeability

After fasting and deprivation of water overnight, rats were gavage-fed with 100 mg/mL of fluorescein isothiocyanate-conjugated dextran (FITC-dextran; 4.4 kDa, catalog FD4, Sigma-Aldrich) at 44 mg/100g of body weight per rat. 4 Hours later, serum was collected from the abdominal aorta under intraperitoneal anesthesia. The concentration of FITC-dextran in serum was analyzed by spectrophotofluorometry with excitation at 485 nm and emission at 528 nm, with reference to a standard of serially diluted FITC-dextran (0, 150, 300, 600, 800, 1,000 μg/mL). Serum lipopolysaccharide (LPS) levels were measured by an ELISA kit (Invitrogen).

Flow cytometry analysis of Th17/Treg cells

Fluorescence-activated cell sorting (FACS) was used to evaluate the frequency (%) of Th17 cells ($CD4^+IL\text{-}17A^+$ cells) and Treg cells ($CD4^+CD25^+Foxp3^+$ cells) in the bone marrow of femur.

Th17 cells

Bone marrow cells were incubated at 37°C for 12 h with DMEM cell high-sugar medium mixed with 10% excellent fetal bovine serum and GolgiPulg (1μg/ml). Single-cell suspensions of bone marrow were then prepared in staining buffer, and 1μL of specific FcR blocker was added to block the nonspecific staining mediated by fluorescent antibody FcR receptor. The cells were then stained with fluorescein-isothiocyanate (FITC)-labeled anti-CD4 antibodies to detect surface markers. After membrane rupture, cells were intracellular stained with phycoerythrin (PE)-labeled anti-IL-17A antibodies. Cells were detected using a flow cytometer (Beckman, FC500, USA).

Treg cells

Single-cell suspensions of bone marrow were prepared in staining buffer. The cells were then stained with FITC-labeled anti-CD4 antibodies, followed by PE anti-CD25 antibodies. After the fixation and membrane rupture, cells were stained with allophycocyanin (APC)-labeled anti-Foxp3 antibodies. Cells were detected using a flow cytometer (Beckman, FC500, USA).

Butyrate treatment

To further validate the role of intestinal butyrate in maintaining gut permeability and preventing skewed Th17/Treg-induced bone resorption, additional OVX/sham rats were gavage-fed with sodium butyrate (400 mg/kg) every day for 8 wk until sacrifice. Serum, ileum and bone marrow cells were collected for further analyses with the same methods as described above.

Statistical analysis

All data were statistically analyzed by SPSS v25.0 (Statistical Product and Service Solutions, International Business Machine Inc, USA). Differences between groups were evaluated by one-way analysis of variance with Bonferroni correction for multiple comparisons or by the Kruskal-Wallis H test with post hoc tests applying the Nemenyi test for multiple comparisons. The data were presented as means ± standard deviation (SD), and a 2-tailed $p < 0.05$ was considered significant.

Table 1. qPCR primer sequences for the TJ protein encoding genes.

Primers	FP (5′ to 3′)	RP (5′ to 3′)
Ocln	GCACGTTCGACCAATGCTCT	AGATGCCCGTTCCATAGGCT
Cldn 1	ACTTTGCAGGCAACCAGAGC	TGCTGTGGCCACTAATGTCG
Cldn2	TCCCCAACTGGCGAACAAGT	AGCGAGGACATTGCACTGGA
Cldn 3	GGCCAGATGCAGTGCAAGAT	CCGAAGGCTGCCAGTAGGAT
Zo 1	TCCCACAAGGAGCCATTCCT	GTCACAGTGTGGCAAGCGT
Jam 3	ACGGTCAGACTCAGCCATCT	AGAGTGCCTGTCTCCGAGTT

Table 2. qPCR primer sequences for butyryl-CoA:acetate CoA transferase and butyrate kinase encoding genes.

Primers	FP (5′ to 3′)	RP (5′ to 3′)
But	GCIGAICATTTCACITGGAAYWSITGGCAYATG	CCTGCCTTTGCAATRTCIACRAANGC
Buk	GTATAGATTACTIRYIATHAAYCCNGG	CAAGCTCRTCIACIACIACNGGRTCNAC

Table 3. qPCR primer sequences for the butyrate-producing genera.

Primers	FP (5’ to 3’)	RP (5’ to 3’)
Clostridium leptum subgroup	CGTCATCCCCACCTTCCTCC	GCAAGACAGTTTCAAGCGCA
Clostridium coccoides subgroup	AATGCCGCGGTGAATACGTT	GCACCTTCCGATACGGCTAC
Fecalibacterium prausnitzii	GATGGCCTCGCGTCCGATTAG	CCGAAGACCTTCTTCCTC
Roseburia/E. rectale cluster	CKGCAAGTCTGATGTGAAAG	GCGGGTCCCCGTCAATTCC

Abbreviations

ANOSIM: analysis of similarity; Adonis: non-parametric multivariate analysis of variance ; AP: apical periodontitis; BMD: bone mineral density; Buk: butyrate kinase; But: butyryl-CoA:acetate CoA transferas; BV/TV: bone volume per tissue; CEJ: cemento-enamel junction; CP: Chronic periodontitis; CTLA-4: cytolytic T lymphocyte associated antigen-4; ELISA: enzyme-linked immunosorbent assay; FITC: fluorescein isothiocyanate; Foxp3: forkheadbox protein 3; HDAC: histone deacetylase; hpf: high-power field; H&E: hematoxylin and eosin; IBD: inflammatory bowel disease; IBS: irritable bowel syndrome; ICD: intestinal crypt depth; IDO: indoleamine 2,3-dioxygenase; IHC: immunohistochemical; IVD: intestinal villus density; IVH: intestinal villus height; LPS: lipopolysaccharides; lsPro; life space probiotics; Micro-CT: micro-computed tomography; MRONJ: medication-related osteonecrosis of the jaw; OCN: osteocalcin; OUT: operational taxonomic unit; OVX: ovariectomized; PBS: phosphate-buffered saline; PCA: Principal components analysis; PCoA: principal coordinates analysis; PMO: postmenopausal osteoporosis; RANKL: receptor activator of nuclear factor-κB ligand; ROI: the region of interest; SCFAs: short chain fatty acids; SD: standard deviation; SPF: specific pathogen free; Tb.N: trabecular number; Tb.Pf: trabecular bone pattern factor; Tb.Sp: trabecular separation; TGF: transforming growth factor; Th: T helper cell; TJ: tight junction; TNF: tumor necrosis factor; TRAP: tartrate-resistant acid phosphatase; Treg: T regulartory cell; Veh: Vehicle; V/C: villus height to crypt depth.

Declarations

Acknowledgments and funding

This study was supported by the National Natural Science Foundation of China (81771099, 81870754, 81800989), research grants from the Science and Technology Department of Sichuan Province (2018SZ0121).

Ethics approval and consent to participate

All animal procedures in this study were approved by the Ethics Committee of West China Hospital, Sichuan University (license number WCHSIRB-D-2018-150).

Consent for publication

Not applicable.

Availability of data and materials

Raw 16S rRNA gene sequences for all samples used in this study were deposited in Sequence Read Archive (https://www.ncbi.nlm.nih.gov/Traces/sra; accession nos. SRP285657).

Competing interests

The authors declare that they have no competing interests.

Authors' contributions

Xin Xu elaborated the study design. Leming Jia and Ye Tu collected the data. Xin Xu, Leming Jia, Ye Tu, Xiaoyue Jia, Du Qian and Xin Zheng contributed to the data analysis. Xin Xu, Ye Tu and Leming Jia were major contributors in writing the manuscript. Xin Xu and Xuedong Zhou contributed to the funding acquisition. All authors read and approved the final manuscript.

References

1. Eastell R, O'Neill TW, Hofbauer LC, Langdahl B, Reid IR, Gold DT, et al. Postmenopausal osteoporosis. Nature reviews Disease primers. 2016;2:16069; doi: 10.1038/nrdp.2016.69.
2. Weitzmann MN, Pacifici R. Estrogen deficiency and bone loss: an inflammatory tale. The Journal of clinical investigation. 2006;116(5):1186-94; doi: 10.1172/jci28550.
3. Mundy GR. Osteoporosis and inflammation. Nutrition reviews. 2007;65(12 Pt 2):S147-51; doi: 10.1111/j.1753-4887.2007.tb00353.x.
4. Luo CY, Wang L, Sun C, Li DJ. Estrogen enhances the functions of CD4(+)CD25(+)Foxp3(+) regulatory T cells that suppress osteoclast differentiation and bone resorption in vitro. Cellular & molecular immunology. 2011;8(1):50-8; doi: 10.1038/cmi.2010.54.
5. Manolagas SC, O'Brien CA, Almeida M. The role of estrogen and androgen receptors in bone health and disease. Nature reviews Endocrinology. 2013;9(12):699-712; doi: 10.1038/nrendo.2013.179.
6. Sapir-Koren R, Livshits G. Postmenopausal osteoporosis in rheumatoid arthritis: The estrogen deficiency-immune mechanisms link. Bone. 2017;103:102-15; doi: 10.1016/j.bone.2017.06.020.
7. Tyagi AM, Srivastava K, Mansoori MN, Trivedi R, Chattopadhyay N, Singh D. Estrogen deficiency induces the differentiation of IL-17 secreting Th17 cells: a new candidate in the pathogenesis of osteoporosis. PloS one. 2012;7(9):e44552; doi: 10.1371/journal.pone.0044552.
8. Li JY, Chassaing B, Tyagi AM, Vaccaro C, Luo T, Adams J, et al. Sex steroid deficiency-associated bone loss is microbiota dependent and prevented by probiotics. The Journal of clinical investigation. 2016;126(6):2049-63; doi: 10.1172/jci86062.
9. Zhao R, Wang X, Feng F. Upregulated Cellular Expression of IL-17 by CD4+ T-Cells in Osteoporotic Postmenopausal Women. Annals of nutrition & metabolism. 2016;68(2):113-8; doi:

10.1159/000443531.

10. DeSelm CJ, Takahata Y, Warren J, Chappel JC, Khan T, Li X, et al. IL-17 mediates estrogen-deficient osteoporosis in an Act1-dependent manner. Journal of cellular biochemistry. 2012;113(9):2895-902; doi: 10.1002/jcb.24165.
11. Molnár I, Bohaty I, Somogyiné-Vári É. IL-17A-mediated sRANK ligand elevation involved in postmenopausal osteoporosis. Osteoporosis international : a journal established as result of cooperation between the European Foundation for Osteoporosis and the National Osteoporosis Foundation of the USA. 2014;25(2):783-6; doi: 10.1007/s00198-013-2548-6.
12. Kotake S, Udagawa N, Takahashi N, Matsuzaki K, Itoh K, Ishiyama S, et al. IL-17 in synovial fluids from patients with rheumatoid arthritis is a potent stimulator of osteoclastogenesis. The Journal of clinical investigation. 1999;103(9):1345-52; doi: 10.1172/jci5703.
13. Yu JJ, Ruddy MJ, Conti HR, Boonanantanasarn K, Gaffen SL. The interleukin-17 receptor plays a gender-dependent role in host protection against Porphyromonas gingivalis-induced periodontal bone loss. Infect Immun. 2008;76(9):4206-13; doi: 10.1128/IAI.01209-07.
14. Yu JJ, Ruddy MJ, Wong GC, Sfintescu C, Baker PJ, Smith JB, et al. An essential role for IL-17 in preventing pathogen-initiated bone destruction: recruitment of neutrophils to inflamed bone requires IL-17 receptor-dependent signals. Blood. 2007;109(9):3794-802; doi: 10.1182/blood-2005-09-010116.
15. Slots J. Periodontitis: facts, fallacies and the future. Periodontology 2000. 2017;75(1):7-23; doi: 10.1111/prd.12221.
16. Nair PN. Apical periodontitis: a dynamic encounter between root canal infection and host response. Periodontology 2000. 1997;13:121-48; doi: 10.1111/j.1600-0757.1997.tb00098.x.
17. Wang CJ, McCauley LK. Osteoporosis and Periodontitis. Current osteoporosis reports. 2016;14(6):284-91; doi: 10.1007/s11914-016-0330-3.
18. Payne JB, Reinhardt RA, Nummikoski PV, Patil KD. Longitudinal alveolar bone loss in postmenopausal osteoporotic/osteopenic women. Osteoporosis international : a journal established as result of cooperation between the European Foundation for Osteoporosis and the National Osteoporosis Foundation of the USA. 1999;10(1):34-40; doi: 10.1007/s001980050191.
19. Du Z, Steck R, Doan N, Woodruff MA, Ivanovski S, Xiao Y. Estrogen Deficiency-Associated Bone Loss in the Maxilla: A Methodology to Quantify the Changes in the Maxillary Intra-radicular Alveolar Bone in an Ovariectomized Rat Osteoporosis Model. Tissue engineering Part C, Methods. 2015;21(5):458-66; doi: 10.1089/ten.TEC.2014.0268.
20. Brasil SC, Santos RMM, Fernandes A, Alves FRF, Pires FR, Siqueira JF, et al. Influence of oestrogen deficiency on the development of apical periodontitis. International Endodontic Journal. 2017;50(2):161-6; doi: 10.1111/iej.12612.
21. Renvert S, Persson GR. Treatment of periodontal disease in older adults. Periodontol 2000. 2016;72(1):108-19; doi: 10.1111/prd.12130.
22. Darby I. Periodontal considerations in older individuals. Aust Dent J. 2015;60 Suppl 1:14-9; doi: 10.1111/adj.12280.

23. Genco RJ, LaMonte MJ, McSkimming DI, Buck MJ, Li L, Hovey KM, et al. The Subgingival Microbiome Relationship to Periodontal Disease in Older Women. J Dent Res. 2019;98(9):975-84; doi: 10.1177/0022034519860449.
24. Xiong H, Peng B, Wei L, Zhang X, Wang L. Effect of an estrogen-deficient state and alendronate therapy on bone loss resulting from experimental periapical lesions in rats. Journal of endodontics. 2007;33(11):1304-8; doi: 10.1016/j.joen.2007.07.011.
25. Beth-Tasdogan NH, Mayer B, Hussein H, Zolk O. Interventions for managing medication-related osteonecrosis of the jaw. The Cochrane database of systematic reviews. 2017;10(10):Cd012432; doi: 10.1002/14651858.CD012432.pub2.
26. Kim J, Lee DH, Dziak R, Ciancio S. Bisphosphonate-related osteonecrosis of the jaw: Current clinical significance and treatment strategy review. American journal of dentistry. 2020;33(3):115-28.
27. Chen Y-C, Greenbaum J, Shen H, Deng H-WJTJoCE, Metabolism. Association between gut microbiota and bone health: potential mechanisms and prospective. 2017;102(10):3635-46.
28. Quach D, Britton RA. Gut microbiota and bone health. In: Understanding the Gut-Bone Signaling Axis. Springer; 2017. p. 47-58.
29. Xu X, Jia X, Mo L, Liu C, Zheng L, Yuan Q, et al. Intestinal microbiota: a potential target for the treatment of postmenopausal osteoporosis. Bone research. 2017;5:17046; doi: 10.1038/boneres.2017.46.
30. Di Stefano M, Veneto G, Malservisi S, Corazza GR. Small intestine bacterial overgrowth and metabolic bone disease. Digestive diseases and sciences. 2001;46(5):1077-82; doi: 10.1023/a:1010722314493.
31. Anantharaju A, Klamut M. Small intestinal bacterial overgrowth: a possible risk factor for metabolic bone disease. Nutrition reviews. 2003;61(4):132-5; doi: 10.1301/nr.2003.apr.132-135.
32. Sjögren K, Engdahl C, Henning P, Lerner UH, Tremaroli V, Lagerquist MK, et al. The gut microbiota regulates bone mass in mice. Journal of bone and mineral research : the official journal of the American Society for Bone and Mineral Research. 2012;27(6):1357-67; doi: 10.1002/jbmr.1588.
33. Pineiro M, Stanton C. Probiotic Bacteria: Legislative Framework— Requirements to Evidence Basis. The Journal of Nutrition. 2007;137(3):850S-3S; doi: 10.1093/jn/137.3.850S %J The Journal of Nutrition.
34. Suez J, Zmora N, Segal E, Elinav E. The pros, cons, and many unknowns of probiotics. Nat Med. 2019;25(5):716-29; doi: 10.1038/s41591-019-0439-x.
35. Pacifici R. Bone Remodeling and the Microbiome. Cold Spring Harbor perspectives in medicine. 2018;8(4); doi: 10.1101/cshperspect.a031203.
36. Yang LC, Lin SW, Li IC, Chen YP, Tzu SY, Chou W, et al. Lactobacillus plantarum GKM3 and Lactobacillus paracasei GKS6 Supplementation Ameliorates Bone Loss in Ovariectomized Mice by Promoting Osteoblast Differentiation and Inhibiting Osteoclast Formation. Nutrients. 2020;12(7); doi: 10.3390/nu12071914.

37. Gatej SM, Marino V, Bright R, Fitzsimmons TR, Gully N, Zilm P, et al. Probiotic Lactobacillus rhamnosus GG prevents alveolar bone loss in a mouse model of experimental periodontitis. J Clin Periodontol. 2018;45(2):204-12; doi: 10.1111/jcpe.12838.
38. Cosme-Silva L, Dal-Fabbro R, Cintra LTA, Dos Santos VR, Duque C, Ervolino E, et al. Systemic administration of probiotics reduces the severity of apical periodontitis. Int Endod J. 2019;52(12):1738-49; doi: 10.1111/iej.13192.
39. Oliveira LF, Salvador SL, Silva PH, Furlaneto FA, Figueiredo L, Casarin R, et al. Benefits of Bifidobacterium animalis subsp. lactis Probiotic in Experimental Periodontitis. Journal of periodontology. 2017;88(2):197-208; doi: 10.1902/jop.2016.160217.
40. Huck O, Mulhall H, Rubin G, Kizelnik Z, Iyer R, Perpich JD, et al. Akkermansia muciniphila reduces Porphyromonas gingivalis-induced inflammation and periodontal bone destruction. J Clin Periodontol. 2020;47(2):202-12; doi: 10.1111/jcpe.13214.
41. Jia X, Jia L, Mo L, Yuan S, Zheng X, He J, et al. Berberine Ameliorates Periodontal Bone Loss by Regulating Gut Microbiota. Journal of dental research. 2019;98(1):107-16; doi: 10.1177/0022034518797275.
42. Juluri R, Prashanth E, Gopalakrishnan D, Kathariya R, Devanoorkar A, Viswanathan V, et al. Association of Postmenopausal Osteoporosis and Periodontal Disease: A Double-Blind Case-Control Study. J Int Oral Health. 2015;7(9):119-23.
43. Segura-Egea JJ, Castellanos-Cosano L, Machuca G, Lopez-Lopez J, Martin-Gonzalez J, Velasco-Ortega E, et al. Diabetes mellitus, periapical inflammation and endodontic treatment outcome. Med Oral Patol Oral Cir Bucal. 2012;17(2):e356-61; doi: 10.4317/medoral.17452.
44. Preshaw PM, Alba AL, Herrera D, Jepsen S, Konstantinidis A, Makrilakis K, et al. Periodontitis and diabetes: a two-way relationship. Diabetologia. 2012;55(1):21-31; doi: 10.1007/s00125-011-2342-y.
45. Behera J, Ison J, Tyagi SC, Tyagi N. The role of gut microbiota in bone homeostasis. Bone. 2020;135:115317; doi: 10.1016/j.bone.2020.115317.
46. Sato K, Suematsu A, Okamoto K, Yamaguchi A, Morishita Y, Kadono Y, et al. Th17 functions as an osteoclastogenic helper T cell subset that links T cell activation and bone destruction. The Journal of experimental medicine. 2006;203(12):2673-82; doi: 10.1084/jem.20061775.
47. Roggia C, Gao Y, Cenci S, Weitzmann MN, Toraldo G, Isaia G, et al. Up-regulation of TNF-producing T cells in the bone marrow: a key mechanism by which estrogen deficiency induces bone loss in vivo. Proceedings of the National Academy of Sciences of the United States of America. 2001;98(24):13960-5; doi: 10.1073/pnas.251534698.
48. Tyagi AM, Mansoori MN, Srivastava K, Khan MP, Kureel J, Dixit M, et al. Enhanced immunoprotective effects by anti-IL-17 antibody translates to improved skeletal parameters under estrogen deficiency compared with anti-RANKL and anti-TNF-alpha antibodies. J Bone Miner Res. 2014;29(9):1981-92; doi: 10.1002/jbmr.2228.
49. Tai P, Wang J, Jin H, Song X, Yan J, Kang Y, et al. Induction of regulatory T cells by physiological level estrogen. Journal of cellular physiology. 2008;214(2):456-64; doi: 10.1002/jcp.21221.

50. Pacifici R. Role of T cells in ovariectomy induced bone loss--revisited. Journal of bone and mineral research : the official journal of the American Society for Bone and Mineral Research. 2012;27(2):231-9; doi: 10.1002/jbmr.1500.
51. Okamoto K, Takayanagi H. Osteoimmunology. Cold Spring Harbor perspectives in medicine. 2019;9(1); doi: 10.1101/cshperspect.a031245.
52. Kim YG, Lee CK, Nah SS, Mun SH, Yoo B, Moon HB. Human CD4+CD25+ regulatory T cells inhibit the differentiation of osteoclasts from peripheral blood mononuclear cells. Biochemical and biophysical research communications. 2007;357(4):1046-52; doi: 10.1016/j.bbrc.2007.04.042.
53. Bozec A, Zaiss MM, Kagwiria R, Voll R, Rauh M, Chen Z, et al. T cell costimulation molecules CD80/86 inhibit osteoclast differentiation by inducing the IDO/tryptophan pathway. Science translational medicine. 2014;6(235):235ra60; doi: 10.1126/scitranslmed.3007764.
54. Hori S, Nomura T, Sakaguchi S. Control of regulatory T cell development by the transcription factor Foxp3. Science. 2003;299(5609):1057-61; doi: 10.1126/science.1079490.
55. Noack M, Miossec P. Th17 and regulatory T cell balance in autoimmune and inflammatory diseases. Autoimmun Rev. 2014;13(6):668-77; doi: 10.1016/j.autrev.2013.12.004.
56. Guo S, Al-Sadi R, Said HM, Ma TY. Lipopolysaccharide causes an increase in intestinal tight junction permeability in vitro and in vivo by inducing enterocyte membrane expression and localization of TLR-4 and CD14. Am J Pathol. 2013;182(2):375-87; doi: 10.1016/j.ajpath.2012.10.014.
57. Dheer R, Santaolalla R, Davies JM, Lang JK, Phillips MC, Pastorini C, et al. Intestinal Epithelial Toll-Like Receptor 4 Signaling Affects Epithelial Function and Colonic Microbiota and Promotes a Risk for Transmissible Colitis. Infect Immun. 2016;84(3):798-810; doi: 10.1128/IAI.01374-15.
58. Parada Venegas D, De la Fuente MK, Landskron G, González MJ, Quera R, Dijkstra G, et al. Short Chain Fatty Acids (SCFAs)-Mediated Gut Epithelial and Immune Regulation and Its Relevance for Inflammatory Bowel Diseases. Frontiers in immunology. 2019;10:277; doi: 10.3389/fimmu.2019.00277.
59. Zheng L, Kelly CJ, Battista KD, Schaefer R, Lanis JM, Alexeev EE, et al. Microbial-Derived Butyrate Promotes Epithelial Barrier Function through IL-10 Receptor-Dependent Repression of Claudin-2. J Immunol. 2017;199(8):2976-84; doi: 10.4049/jimmunol.1700105.
60. Asarat M, Apostolopoulos V, Vasiljevic T, Donkor O. Short-Chain Fatty Acids Regulate Cytokines and Th17/Treg Cells in Human Peripheral Blood Mononuclear Cells in vitro. Immunological investigations. 2016;45(3):205-22; doi: 10.3109/08820139.2015.1122613.
61. Luu M, Pautz S, Kohl V, Singh R, Romero R, Lucas S, et al. The short-chain fatty acid pentanoate suppresses autoimmunity by modulating the metabolic-epigenetic crosstalk in lymphocytes. Nature communications. 2019;10(1):760; doi: 10.1038/s41467-019-08711-2.
62. Arpaia N, Campbell C, Fan X, Dikiy S, van der Veeken J, deRoos P, et al. Metabolites produced by commensal bacteria promote peripheral regulatory T-cell generation. Nature. 2013;504(7480):451-5; doi: 10.1038/nature12726.

63. Furusawa Y, Obata Y, Fukuda S, Endo TA, Nakato G, Takahashi D, et al. Commensal microbe-derived butyrate induces the differentiation of colonic regulatory T cells. Nature. 2013;504(7480):446-50; doi: 10.1038/nature12721.
64. Chambers ES, Preston T, Frost G, Morrison DJ. Role of Gut Microbiota-Generated Short-Chain Fatty Acids in Metabolic and Cardiovascular Health. Curr Nutr Rep. 2018;7(4):198-206; doi: 10.1007/s13668-018-0248-8.
65. Ho L, Ono K, Tsuji M, Mazzola P, Singh R, Pasinetti GM. Protective roles of intestinal microbiota derived short chain fatty acids in Alzheimer's disease-type beta-amyloid neuropathological mechanisms. Expert Rev Neurother. 2018;18(1):83-90; doi: 10.1080/14737175.2018.1400909.
66. Rosser EC, Piper CJM, Matei DE, Blair PA, Rendeiro AF, Orford M, et al. Microbiota-Derived Metabolites Suppress Arthritis by Amplifying Aryl-Hydrocarbon Receptor Activation in Regulatory B Cells. Cell Metab. 2020;31(4):837-51 e10; doi: 10.1016/j.cmet.2020.03.003.
67. Ulluwishewa D, Anderson RC, McNabb WC, Moughan PJ, Wells JM, Roy NC. Regulation of tight junction permeability by intestinal bacteria and dietary components. J Nutr. 2011;141(5):769-76; doi: 10.3945/jn.110.135657.
68. Wang J, Ji H, Wang S, Liu H, Zhang W, Zhang D, et al. Probiotic Lactobacillus plantarum Promotes Intestinal Barrier Function by Strengthening the Epithelium and Modulating Gut Microbiota. Frontiers in microbiology. 2018;9:1953; doi: 10.3389/fmicb.2018.01953.
69. den Besten G, van Eunen K, Groen AK, Venema K, Reijngoud DJ, Bakker BM. The role of short-chain fatty acids in the interplay between diet, gut microbiota, and host energy metabolism. J Lipid Res. 2013;54(9):2325-40; doi: 10.1194/jlr.R036012.
70. Scholz-Ahrens KE, Ade P, Marten B, Weber P, Timm W, Acil Y, et al. Prebiotics, probiotics, and synbiotics affect mineral absorption, bone mineral content, and bone structure. J Nutr. 2007;137(3 Suppl 2):838s-46s; doi: 10.1093/jn/137.3.838S.
71. Rodrigues FC, Castro AS, Rodrigues VC, Fernandes SA, Fontes EA, de Oliveira TT, et al. Yacon flour and Bifidobacterium longum modulate bone health in rats. Journal of medicinal food. 2012;15(7):664-70; doi: 10.1089/jmf.2011.0296.
72. Britton RA, Irwin R, Quach D, Schaefer L, Zhang J, Lee T, et al. Probiotic L. reuteri treatment prevents bone loss in a menopausal ovariectomized mouse model. Journal of cellular physiology. 2014;229(11):1822-30; doi: 10.1002/jcp.24636.
73. Ohlsson C, Engdahl C, Fåk F, Andersson A, Windahl SH, Farman HH, et al. Probiotics protect mice from ovariectomy-induced cortical bone loss. PloS one. 2014;9(3):e92368; doi: 10.1371/journal.pone.0092368.
74. Dar HY, Shukla P, Mishra PK, Anupam R, Mondal RK, Tomar GB, et al. Lactobacillus acidophilus inhibits bone loss and increases bone heterogeneity in osteoporotic mice via modulating Treg-Th17 cell balance. Bone reports. 2018;8:46-56; doi: 10.1016/j.bonr.2018.02.001.
75. Alshareef A, Attia A, Almalki M, Alsharif F, Melibari A, Mirdad B, et al. Effectiveness of Probiotic Lozenges in Periodontal Management of Chronic Periodontitis Patients: Clinical and Immunological

Study. European journal of dentistry. 2020;14(2):281-7; doi: 10.1055/s-0040-1709924.

76. Cosme-Silva L, Dal-Fabbro R, Cintra LTA, Ervolino E, Plazza F, Mogami Bomfim S, et al. Reduced bone resorption and inflammation in apical periodontitis evoked by dietary supplementation with probiotics in rats. Int Endod J. 2020; doi: 10.1111/iej.13311.
77. Ho SN, Acharya A, Sidharthan S, Li KY, Leung WK, McGrath C, et al. A Systematic Review and Meta-analysis of Clinical, Immunological, and Microbiological Shift in Periodontitis After Nonsurgical Periodontal Therapy With Adjunctive Use of Probiotics. The journal of evidence-based dental practice. 2020;20(1):101397; doi: 10.1016/j.jebdp.2020.101397.
78. Collins FL, Irwin R, Bierhalter H, Schepper J, Britton RA, Parameswaran N, et al. Lactobacillus reuteri 6475 Increases Bone Density in Intact Females Only under an Inflammatory Setting. PloS one. 2016;11(4):e0153180; doi: 10.1371/journal.pone.0153180.
79. Zmora N, Zilberman-Schapira G, Suez J, Mor U, Dori-Bachash M, Bashiardes S, et al. Personalized Gut Mucosal Colonization Resistance to Empiric Probiotics Is Associated with Unique Host and Microbiome Features. Cell. 2018;174(6):1388-405 e21; doi: 10.1016/j.cell.2018.08.041.
80. Bunyavanich S. Food allergy: could the gut microbiota hold the key? Nature reviews Gastroenterology & hepatology. 2019;16(4):201-2; doi: 10.1038/s41575-019-0123-0.
81. Flores R, Shi J, Fuhrman B, Xu X, Veenstra TD, Gail MH, et al. Fecal microbial determinants of fecal and systemic estrogens and estrogen metabolites: a cross-sectional study. Journal of translational medicine. 2012;10:253; doi: 10.1186/1479-5876-10-253.
82. Li CH, Amar S. Inhibition of SFRP1 reduces severity of periodontitis. Journal of dental research. 2007;86(9):873-7; doi: 10.1177/154405910708600913.
83. Aksoy U, Savtekin G, Şehirli AÖ, Kermeoğlu F, Kalender A, Özkayalar H, et al. Effects of alpha-lipoic acid therapy on experimentally induced apical periodontitis: a biochemical, histopathological and micro-CT analysis. International Endodontic Journal. 2019;52(9):1317-26; doi: 10.1111/iej.13121.
84. Yang S, Zhu L, Xiao L, Shen Y, Wang L, Peng B, et al. Imbalance of interleukin-17+ T-cell and Foxp3+ regulatory T-cell dynamics in rat periapical lesions. Journal of endodontics. 2014;40(1):56-62; doi: 10.1016/j.joen.2013.09.033.

Figures

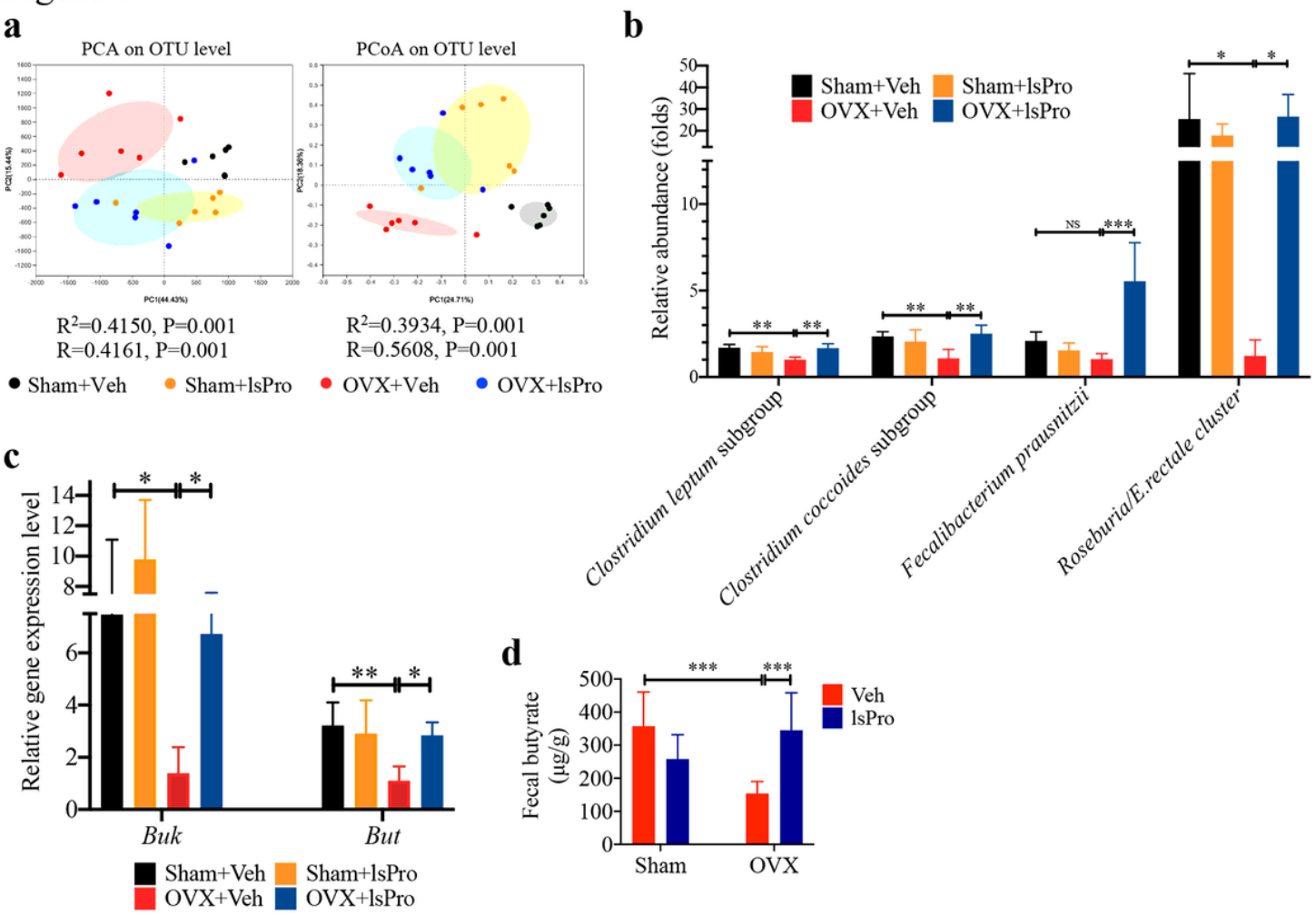

Figure 1

Probiotics enrich butyrate-producing gut microbiota in OVX rats. (a) The β-diversity analyses (PCA and PCoA) of gut microbial community based on Bray-Curtis distance. (b) The abundance of butyrate-producing genera relative to control (OVX+Veh) as quantified by qPCR. (c) The relative expression levels of butyryl-CoA:acetate CoA transferase and butyrate kinase of the gut microbiota as quantified by qPCR. (d) Quantification of fecal butyrate concentration by HPLC. Data are presented as the mean ± SD, n = 5-8 rats per group, *p < 0.05, **p < 0.01, ***p <0.001. But: butyryl-CoA:acetate CoA transferase; Buk: butyrate kinase; lsPro: life space probiotics; OUT: operational taxonomic unit; PCA: Principal components analysis; PCoA: principal coordinates analysis; Veh: Vehicle.

Figure 2

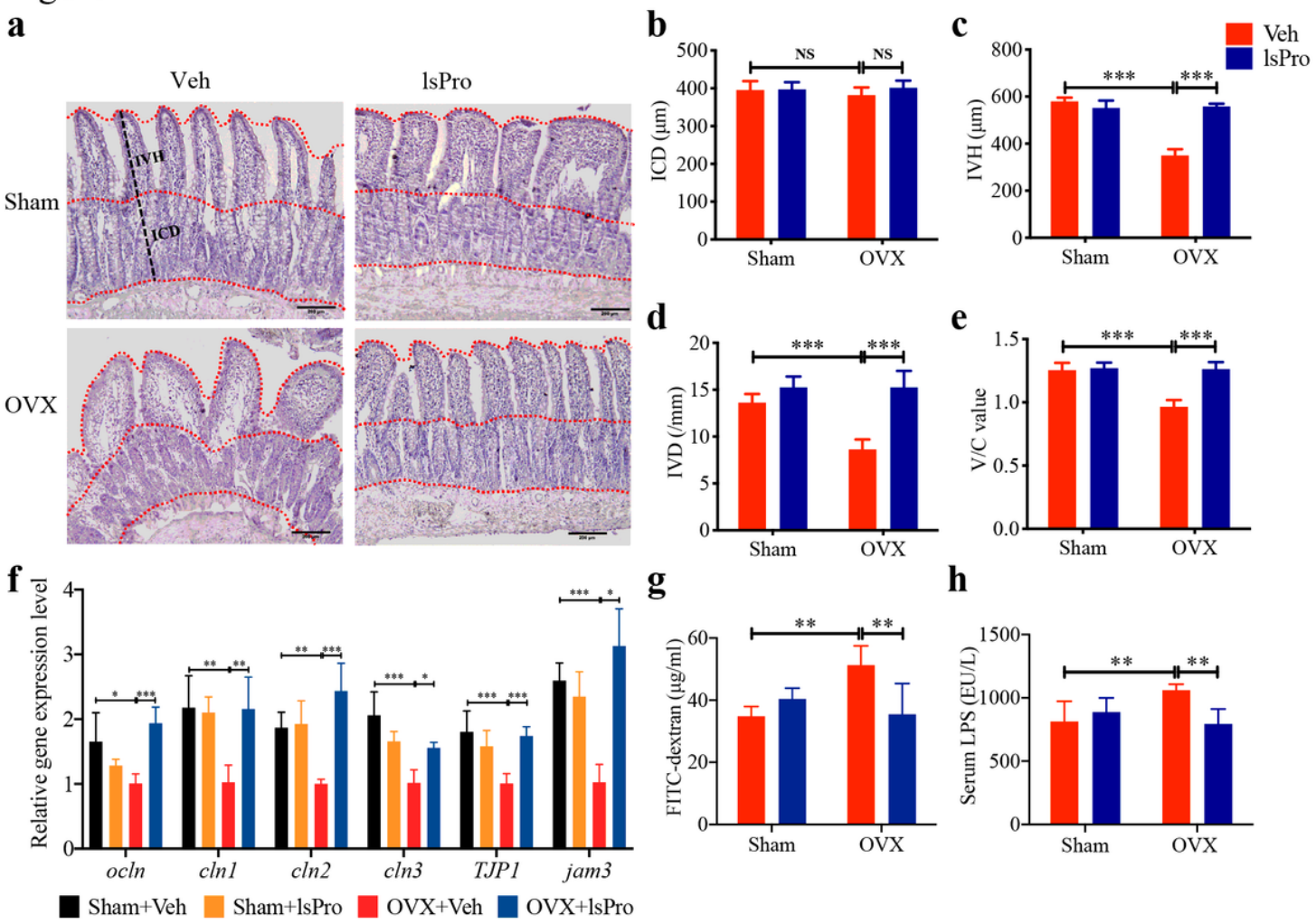

Figure 2

Probiotics restore the gut permeability of OVX rats. (a) Representative images of H&E staining of the ileum mucosa (scale bar = 200 μm). (b-e) Quantitative analyses of ICD, IVD, IVH, and V/C value of the ileum mucosa, respectively. (f) The relative expression levels of intestinal epithelial tight junction proteins as quantified by qPCR. (g) The serum level of FITC-dextran as determined by spectrophotofluorometry. (h) The serum level of LPS as determined by ELISA. Data are presented as the mean ± SD, n = 5-8 rats per group, *p < 0.05, **p < 0.01, ***p <0.001, NS, not significant. ICD: Intestinal crypt depth; IVD: Intestinal villus depth; IVH: Intestinal villus height; lsPro: life space probiotics; Veh: Vehicle; V/C, villus height to crypt depth.

Figure 3

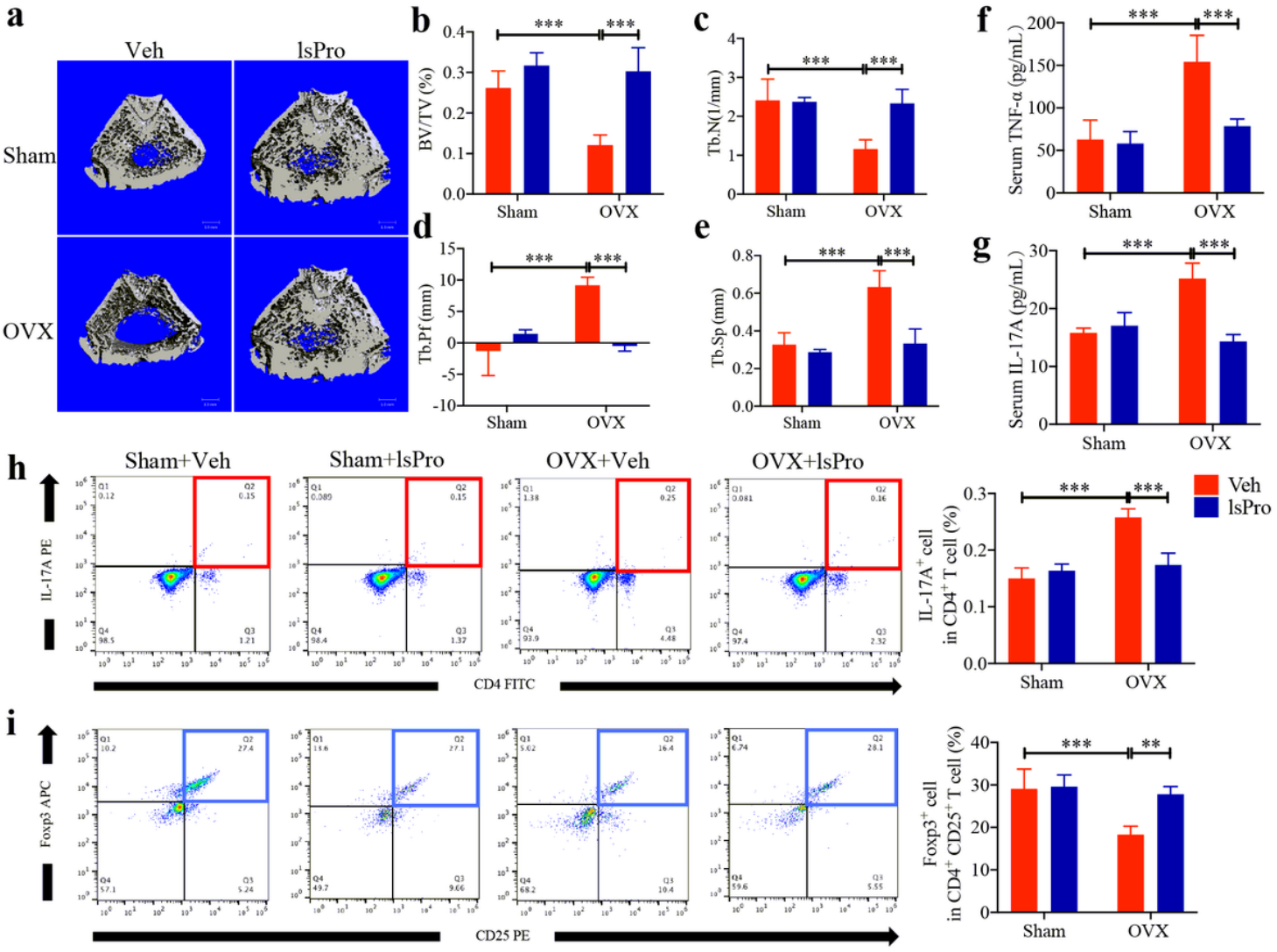

Figure 3

Probiotics ameliorate bone loss and rescue Th17/Treg imbalance in OVX rats. (a) Micro-CT reconstruction of femoral bone structure. (b-e) Quantitative analyses of BV/TV, Tb.N, Tb.Pf, Tb.Sp of the femoral bone by micro-CT. (f) Serum level of IL17-A. (g) Serum level of TNF-α. (h) Representative FACS plots of Th17 cells in the CD4+ T cell subset of the BM and quantitative analysis. (i) Representative FACS plots of Treg cells in CD4+CD25+ T cell subset of the BM and quantitative analysis. Data are presented as the mean ± SD, n = 5-8 rats per group, **p < 0.01, ***p <0.001. BV/TV: bone volume per tissue volume; lsPro: life space probiotics; Tb.N: trabecular number; Tb.Pf: trabeculae pattern factor; Tb.Sp: trabecular separation; Veh, Vehicle.

Figure 4

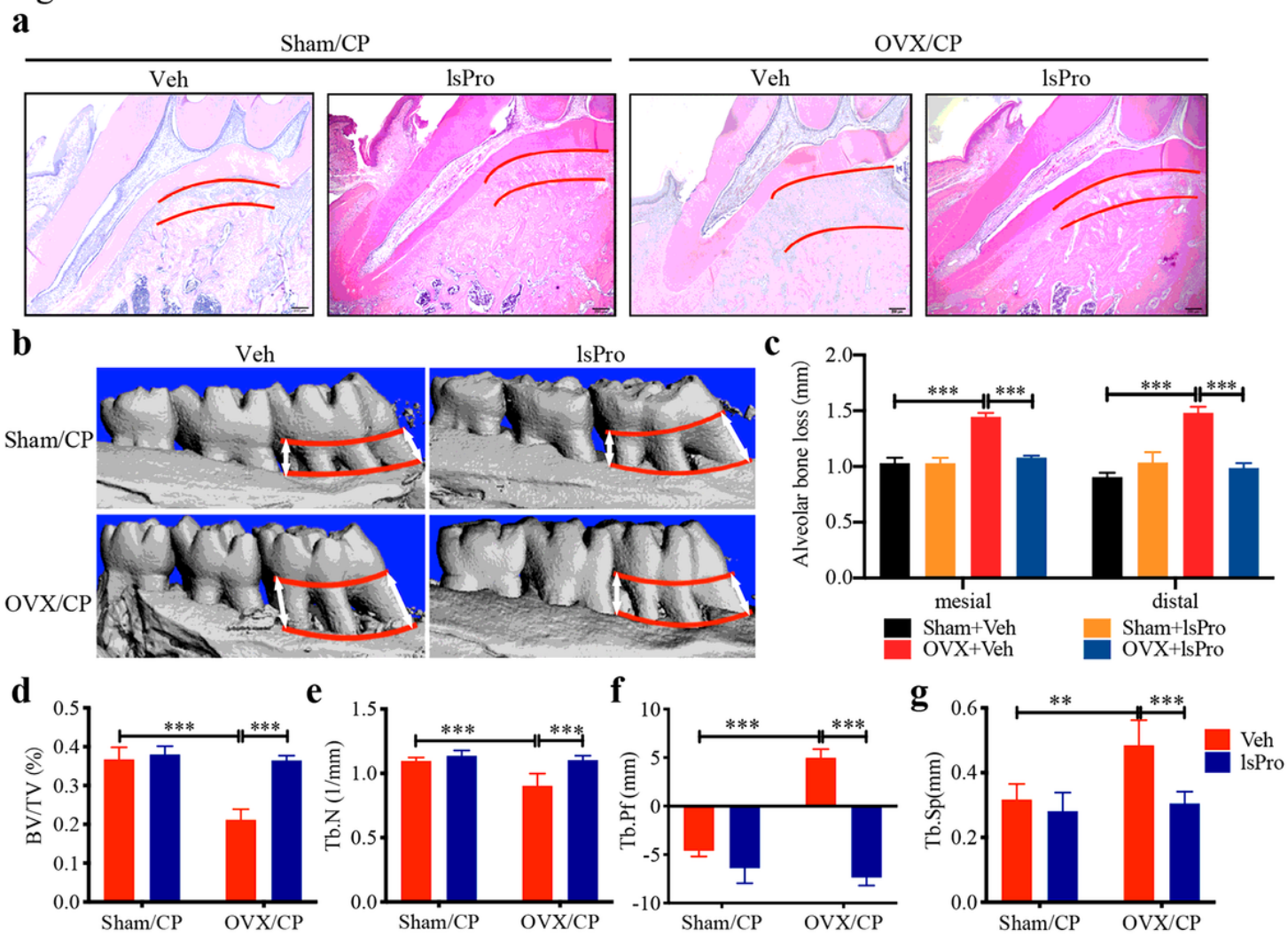

Figure 4

Probiotics ameliorate periodontal bone loss in OVX rats. (a) H&E staining of the alveolar bone loss at root furcation (distance between the red lines). Scale bar = 200 μm. (b) Micro-CT reconstruction of alveolar bone loss between the mesial and distal sites (distance between the red lines) of maxillary first molars. (c) Quantitative analyses of mesial and distal alveolar bone loss by micro-CT. (d-g) Micro-CT analyses of BV/TV, Tb.N, Tb.Pf, and Tb.Sp of the alveolar bone, respectively. Data are presented as the mean ± SD, n = 5-8 rats per group, **p < 0.01, ***p <0.001. BV/TV, bone volume per tissue volume; CP, chronic periodontitis; lsPro, life space probiotics; Tb.N, trabecular number; Tb.Pf, trabeculae pattern factor; Tb.Sp, trabecular separation; Veh, Vehicle.

Figure 5

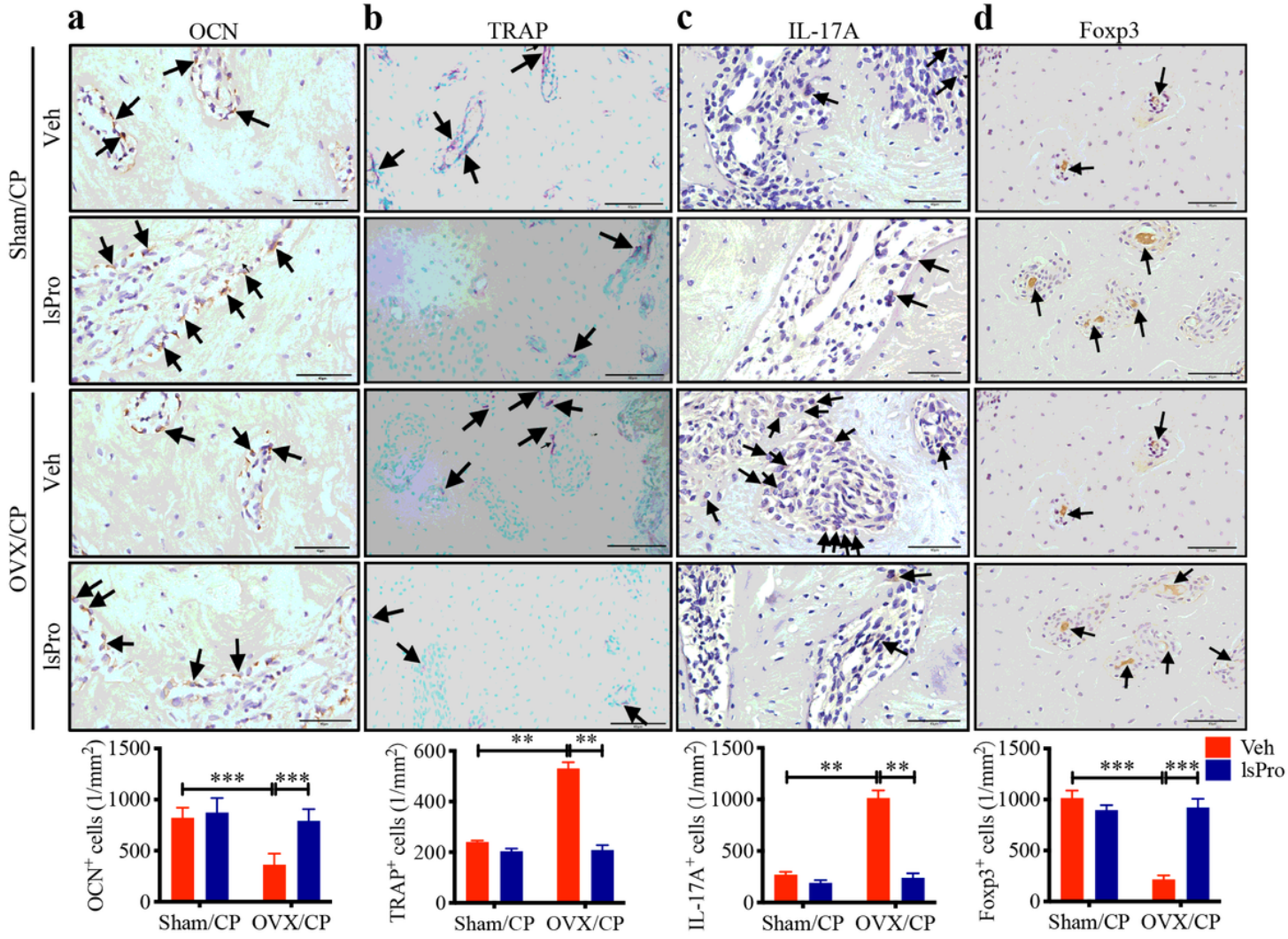

Figure 5

Probiotics attenuate periodontal bone resorption in OVX rats. (a-d) Representative images of OCN+ cells, TRAP+ cells, IL-17A+ cells and Foxp3+ cells at the first molar and quantitative analyses, respectively. Black arrows indicate positively stained cells. Scale bar = 40 μm. Data are presented as the mean ± SD, n = 5-8 rats per group, **p < 0.01, ***p <0.001. CP: chronic periodontitis; IHC: immunohistochemical; lsPro: life space probiotics; OCN: osteocalcin; TRAP: tartrate-resistant acid phosphatase; Veh: Vehicle.

Figure 6

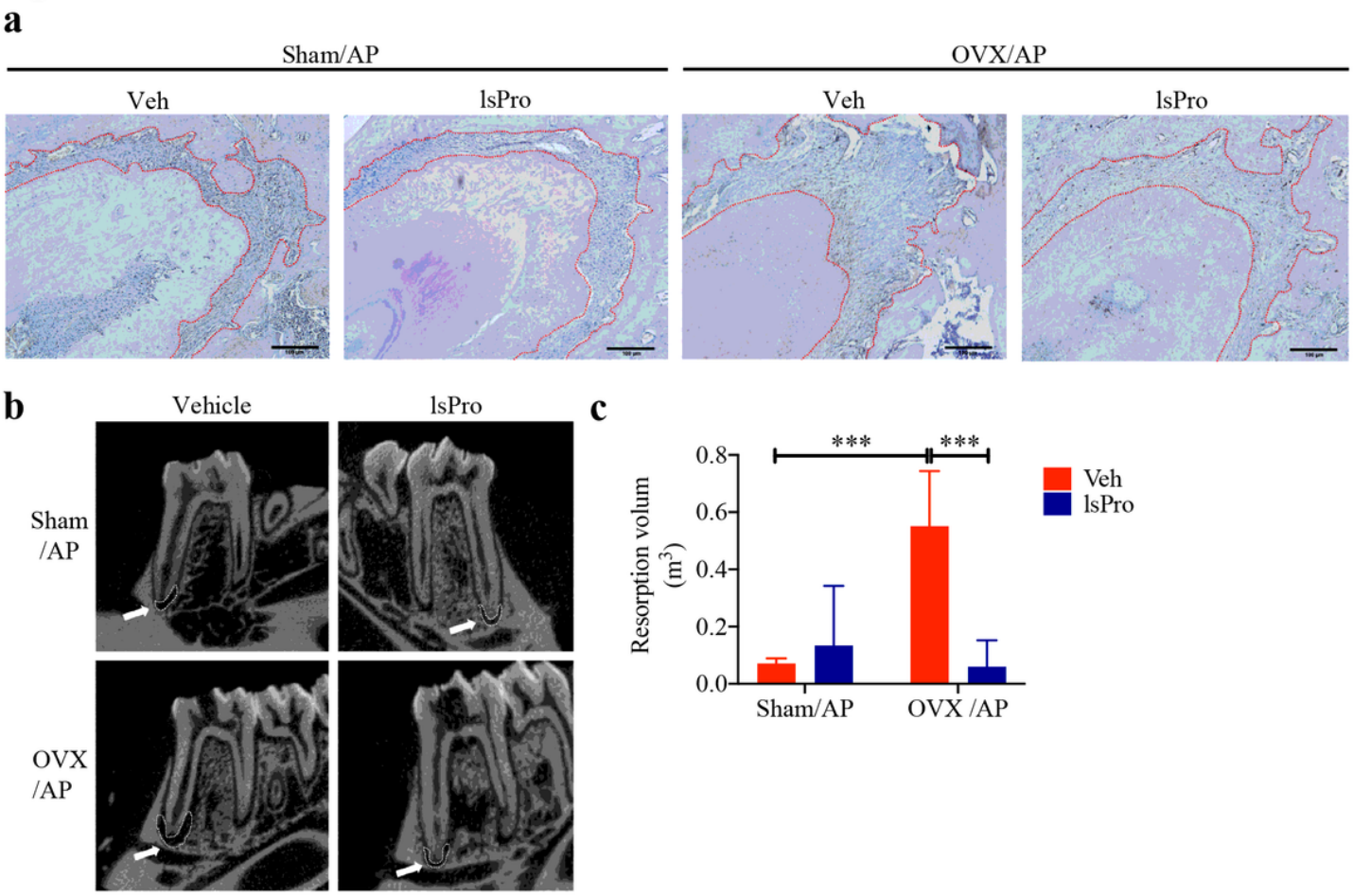

Figure 6

Probiotics ameliorate periapical bone loss in OVX rats. (a) H&E staining indicating alveolar bone loss at apical region (red line). Scale bar = 100 μm. (b, c) Representative micro-CT images of apical lesion (white arrow), and quantitative analysis of resorption volume in apical regions. Data are presented as the mean ± SD, n = 5~8 rats per group, ***p <0 .001. AP, apical periodontitis; lsPro, life space probiotics; Veh, Vehicle.

Figure 7

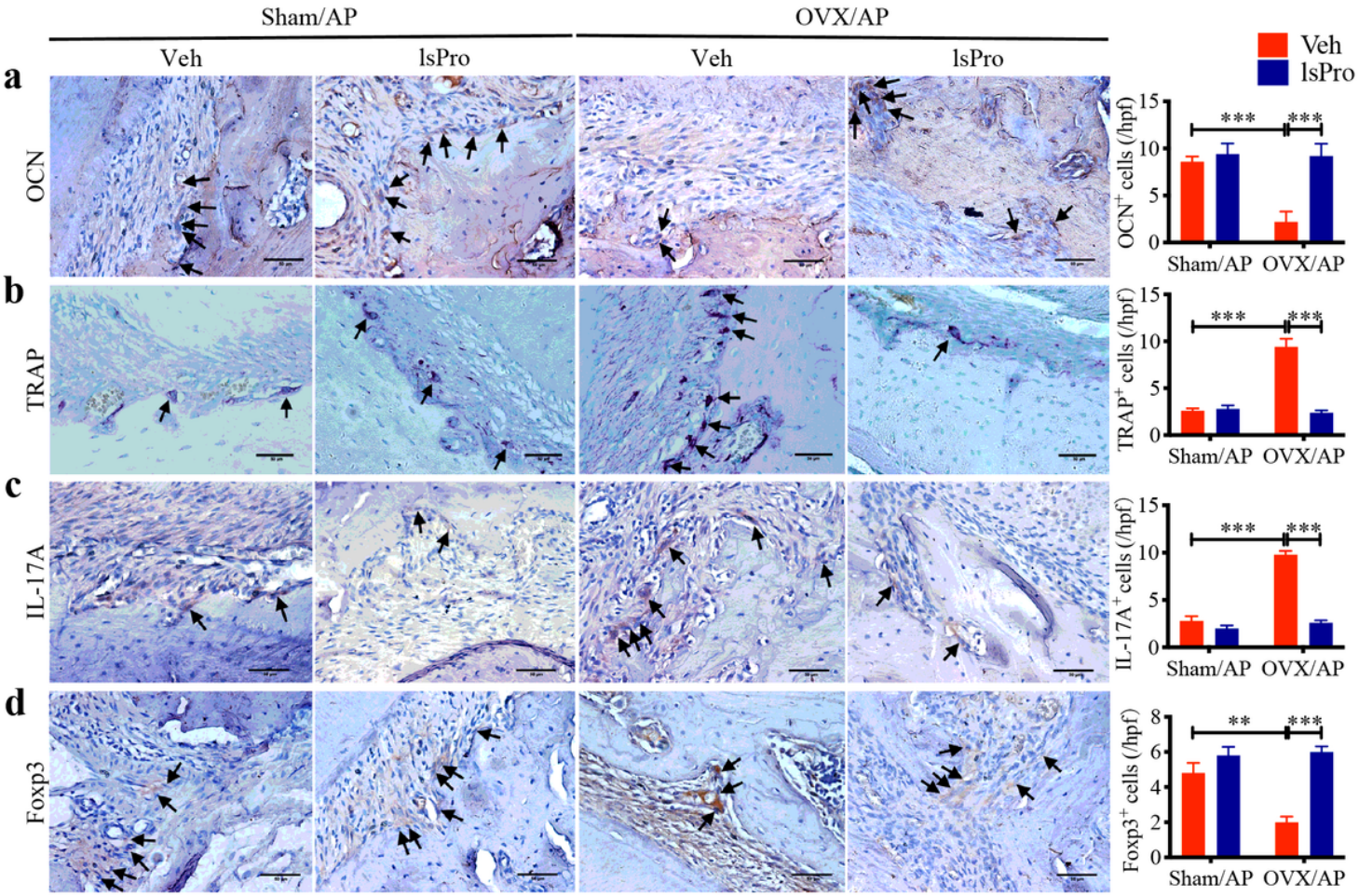

Figure 7

Probiotics attenuate periapical bone resorption in OVX rats. (a-d) Representative images of OCN+ cells, TRAP+ cells, IL-17A+ cells and Foxp3+ cells at the apical area of first molar and quantitative analyses, respectively. Black arrows indicate positively stained cells. Scale bar = 50 μm. Data are presented as the mean ± SD, n = 5~8 rats per group, **p < 0.01, ***p <0 .001. AP, apical periodontitis; Hpf, high power fields; IHC, immunohistochemical; lsPro, life space probiotics; OCN, osteocalcin; TRAP, tartrate-resistant acid phosphatase; Veh, Vehicle.

Supplementary Files

This is a list of supplementary files associated with this preprint. Click to download.

- SupplementaryMaterial.pdf